Crossflow transition modelling for a marine propeller at model scale

25th Numerical Towing Tank Symposium (NuTTS)
15-17 October 2023 - Ericeira, Portugal

Crossflow transition modelling for a marine propeller at model scale

Rui Lopes*, Arash Eslamdoost*, Rikard Johansson†, Seemontini RoyChoudhury† and Rickard E. Bensow*

*Chalmers University of Technology, Gothenburg/Sweden, †Kongsberg Hydrodynamic Research Centre, Kristinehamn/Sweden

rui.lopes@chalmers.se

1 Introduction

One of the options to obtain the performance of a propeller at full scale is to extrapolate from data obtained from model scale testing. The Reynolds number of the model scale experiments typically leads to non-negligible extent of both laminar and turbulent flow, unless the flow is tripped, having a significant impact on the propeller performance. When using Computational Fluid Dynamics (CFD) methods to simulate the flow at model scale, the modelling of laminar to turbulent transition and its most important triggering mechanisms is critical in order to achieve accurate results.

The transition of laminar to turbulent flow is due to the instability of the laminar boundary layer with regards to disturbances that are present in the flow. Depending on the amplitude of these perturbations, different transition mechanisms take place, such as natural or bypass transition. In addition, flow separation can also lead to transition. While the previous effects all can be considered as existing in two-dimensional flows, some only occur in three-dimensional flows, like crossflow transition. This mechanism occurs due to the instability of the crossflow velocity profile and is generally important in surfaces with pronounced curvature, with such a case being propeller blades.

Well established turbulence models used with the Reynolds-averaged Navier-Stokes (RANS) equations, e.g. the Spalart-Allmaras or $k-\omega$ models, fail at accurately predicting transition, since their calibration is done for high Reynolds numbers flows. These models lead to a negligible extent of laminar flow, even at moderate Reynolds numbers of around $10^5 - 10^6$. To accurately predict transition in RANS simulations, transition models are required. The most used transition models in CFD nowadays, such as the $\gamma - Re_\theta$ and γ models, handle some of the aforementioned transition mechanisms such as natural, bypass and separation-induced transition. However, their original formulation was not designed to account for crossflow transition, and is unable to predict transition occuring due to this phenomena. Nonetheless, several extensions to the models have been proposed in the literature to address this shortcoming.

The goal of this work is to demonstrate the importance of crossflow transition modelling for a model scale marine propeller and how it impacts the propeller performance across a range of varying advance coefficients. Simulations for a controllable pitch propeller using the RANS equations with the $k-\omega$ Shear Stress Transport (SST) turbulence model and the γ transition model will be performed. The results from using two alternative crossflow extensions are compared in terms of propeller performance and flow over the blade surface. Baseline computations without crossflow modelling are included as well.

2 Mathematical Formulation

This paper deals with the single-phase flow of a Newtonian, incompressible fluid around a propeller in an open-water setup, described by the RANS equations. The equations are solved in a propeller-fixed reference frame, meaning that the flow can be considered as statistically steady. The computation of the Reynolds stresses, introduced due to Reynolds averaging procedure, is done through Boussinesq's hypothesis and the use of the $k-\omega$ SST eddy-viscosity model. It includes two transport equations, one for the turbulence kinetic energy k, and one for the specific dissipation rate ω.

It is worth noting that the specific implementation of the $k-\omega$ SST model used in this work does not include a production limiter explicitly in the production term of the transport equation of k, like the dissipation based limiter of Menter et al. (2003). Instead, to avoid excess levels of the eddy-viscosity in

stagnation regions, there is a limiter acting directly on the eddy-viscosity μ_t, defined as

$$\mu_t = \rho k \min\left(\frac{1}{\max\left(\omega, (SF_2)/0.31\right)}, \frac{0.6}{\sqrt{3}S}\right), \tag{1}$$

where ρ is the density of the fluid, S is the mean strain-rate magnitude and F_2 is a blending function of the model. The limiter used here can result in slight differences regarding the prediction of transition, as the production limiter used in the SST model can influence the predicted location of transition as shown by Lopes (2021). The remainder of the formulation of the $k-\omega$ SST model is out of the scope of the present paper and can be found in Menter et al. (2003).

In order to correctly account for the effects of laminar to turbulent transition, the γ transition model is used. The model solves one transport equation for the intermittency γ, which represents the fraction of time in which the flow at a given point in the domain is turbulent. The production term of this transport equation, P_γ, is written as

$$P_\gamma = F_{length}\rho S F_{onset}\gamma(1-\gamma), \tag{2}$$

in which F_{length} is a constant and F_{onset} is a function responsible for triggering the production term. The original formulation of the model, which does not account for crossflow transition, can be found in Menter et al. (2015). In order to incorporate the effects of crossflow transition, two different crossflow extensions to the γ model are considered. The first one is the default term available in STAR-CCM+, which modifies F_{onset} to be

$$F_{onset} = \max\left(F_{onset,orig}, F_{onset,SCF}\right), \tag{3}$$

where $F_{onset,orig}$ is the original definition of F_{onset} used in the γ model and $F_{onset,SCF}$ is defined as

$$F_{onset,SCF} = \min\left[\max\left(\frac{\left(2-0.5\frac{h}{0.25\times10^{-6}}\right)\frac{\Omega_s d}{|U_i|}\left(1+\min\left(\frac{\mu_t}{\mu},0.4\right)\right)Re_{\theta c}}{Re^*_{\delta 2t}}, 0\right), 1\right]. \tag{4}$$

In this equation, h is the crossflow-inducing roughness height, d is the nearest wall distance, $|U_i|$ is the magnitude of the mean[1] velocity, $Re_{\theta c}$ is the critical Reynolds number given in the formulation of the γ model and Ω_s is the streamwise helicity defined as

$$\Omega_s = \left|\frac{U_i}{|U_i|}\cdot W_i\right|, \tag{5}$$

in which W_i is the mean vorticity. Finally, $Re^*_{\delta 2t}$ is the crossflow displacement thickness Reynolds number, given by

$$Re^*_{\delta 2t} = \begin{cases} \frac{300}{\pi}\arctan\left[\frac{0.106}{(H-2.3)^{2.05}}\right] & , \quad 2.3 \le H < 2.7 \\ 150 & , \quad H < 2.3 \end{cases} \tag{6}$$

where the shape factor H is obtained from

$$H = 2 + 4.14l - 83.5l^2 + 854l^3 - 3337l^4 + 4576l^5, \tag{7}$$

with $l = 0.25 - \lambda_{\theta L}$, in which $\lambda_{\theta L}$ is the pressure gradient parameter of the γ model.

The second crossflow extension used in this work is also based on the helicity of the flow and was originally developed by Grabe et al. (2015) for the $\gamma - Re_\theta$ transition model. Nonetheless, it has been applied to the γ model before, and the full details of the formulation are given in Lopes (2021), so they are not reproduced here.

It must be mentioned that similarly to the $\gamma - Re_\theta$ model for which they were developed, the two crossflow terms used herein are not Galilean invariant since they depend on the helicity and explicitly use the velocity vector in their formulation. The immediate consequence of this is that the solution will depend on the reference frame being considered. Thus, the direct application of these terms in a case

[1] Since the flow is steady, mean quantities are time-averaged.

such as the flow around a propeller where the body-fixed reference frame is used results in an incorrect application of the model. In order to circumvent this effect, the transport equation for γ is reconstructed in STAR-CCM+ using an equation for a passive scalar and adding the correct source terms. In this approach, the calculation of the helicity uses the velocity relative to the wall, which is a correct application of the model. This approach was tested for the flow around a prolate spheroid using the two different approaches for the motion of the fluid (specification of the velocity at the inlet or imposing the motion through a moving reference frame) to ensure that the correction was working properly.

3 Test case description

The geometry considered in this work is a four-bladed controllable pitch propeller at model scale. The computational domain is a cylinder of radius $30D$ in which D is the propeller diameter. At the inlet, which is located $30D$ away from the propeller plane, the velocity is specified, along with k, ω and γ. The outlet is located $30D$ away from the propeller plane, and the pressure is set at this boundary. The outer boundary of the cylinder is set to a symmetry boundary condition. The boundary condition on the surface of the propeller is a solid wall, with direct application of the no-slip condition.

The computational domain is divided into two connecting but non-overlapping regions: one inner region containing the propeller, in which the moving reference frame approach is used, and another outer region in which the equations are solved in the earth fixed reference frame. The Reynolds number of the flow based on the blade chord length at 70% of the propeller radius and the corresponding velocity ranges from 7.5×10^5 to 8.0×10^5, and the advance coefficients addressed in this study vary from $J = 0.34$ to $J = 0.992$. The turbulence intensity at the inlet is specified to 1% and the eddy-viscosity ratio to 1. The influence of the inlet values of these quantities on the prediction of transition is not studied here.

A set of five grids is used throughout this work in order to assess the numerical uncertainty of the simulations based on the procedure developed by Eça and Hoekstra (2014). The γ transition model can be very sensitive to the discretization error and grid quality as shown by Lopes (2021), and therefore such a study is indispensable to ensure that the solution is not being dominated by numerical errors. The coarsest grid is illustrated in Figure 1. The total number of cells in the computational domain ranges from 6.7M to 45.2M, and the number of surfaces faces on the propeller blades from 75k to 234k.

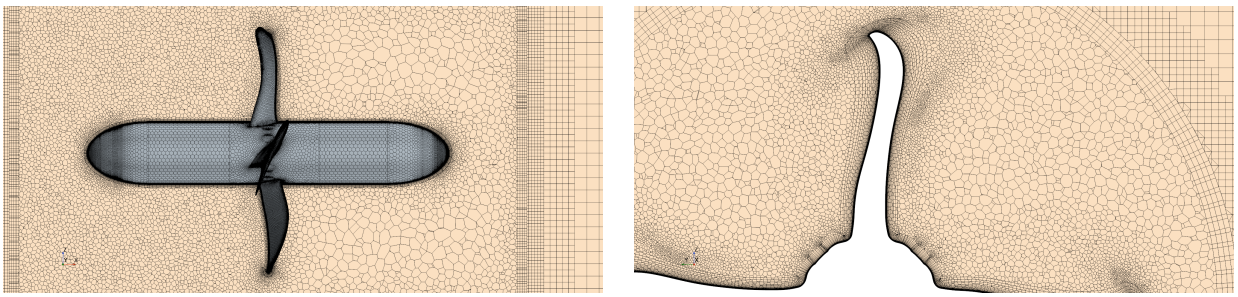

Fig. 1: Illustration of the coarsest grid around the propeller (left) and on the propeller plane (right).

All simulations are carried out using the commercial CFD software STAR-CCM+ 2022.1.1, which uses the finite volume method and the SIMPLE algorithm. The segregated flow solver is used for the solution of the system of equations, and second order discretization schemes are used for the convection term of all transport equations. The simulations performed without any crossflow term are referred to as the γ model, while those performed with the crossflow term of STAR-CCM+ are referred to as $\gamma + CF1$ and the extension of Grabe et al. (2015) is identified as $\gamma + CF2$.

4 Results

The discussion of the results starts with an overview of the iterative convergence of the simulations performed in this study, as it is known from other studies (for example Baltazar et al. (2018)) that transition models are not as robust as turbulence models. Figure 2 illustrates the convergence of the L_∞ norm of the residuals, normalized such that they represent the dimensionless variable change in a simple Jacobi

iteration, for two simulations on the coarsest grid and $J = 0.508$, one without any crossflow term and another with the crossflow term of Grabe et al. (2015). Although the level at which residual stagnation occurs changes from case to case, the trends are representative of all the simulations performed, with the residual of γ stagnating several orders of magnitude higher than the remaining ones. Another observation is that the simulations with a crossflow term typically exhibit better convergence than those without any crossflow term, due to lower extent of separated flow, as will be shown. The level at which stagnation occurs for the residual of the intermittency transport equation depends on the crossflow term employed.

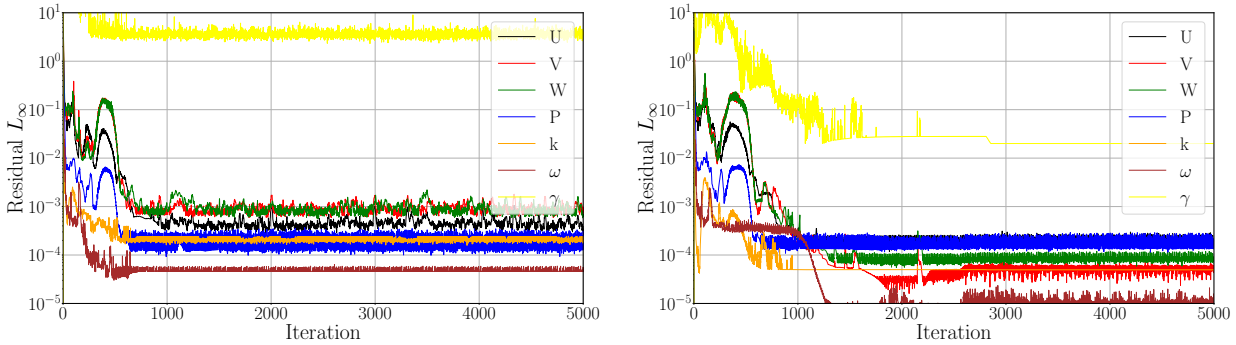

Fig. 2: Evolution of the L_∞ norm of the residuals on the coarsest grid and $J = 0.508$ for a simulation without the crossflow term (left) and with the crossflow term (right).

The results obtained from the grid refinement study for the propeller thrust and torque for each advance coefficient and alternative transition models are given in Table 1. For all models the numerical uncertainty of the thrust and torque coefficients tends to increase with the increase of J. This is both due to the decrease of thrust and torque for each J, as well as a slight increase of the absolute value of the uncertainty. The increase of the uncertainty is much more noticeable for the simulations performed with the $\gamma + CF2$ model. Although including a crossflow term in the model leads overall to more robust simulations regarding iterative convergence, they seem to lead to slightly higher numerical uncertainty than the simulations performed without any crossflow term.

Table 1: Estimate of the numerical uncertainty arising from the discretization error of the finest grid for $10K_Q$ and K_T for different advance coefficients.

J	-	0.34	0.425	0.508	0.588	0.67	0.751	0.835	0.914	0.992
K_T	γ	5.7%	1.6%	1.9%	3.5%	2.0%	2.0%	5.2%	4.6%	41.4%
	$\gamma + CF1$	1.3%	1.7%	2.9%	2.1%	4.8%	6.0%	7.8%	8.3%	22.1%
	$\gamma + CF2$	0.8%	2.0%	2.5%	3.5%	4.4%	5.9%	10.6%	22.5%	159.8%
$10K_Q$	γ	12.7%	4.1%	2.8%	2.1%	3.8%	3.9%	14.8%	8.5%	21.4%
	$\gamma + CF1$	5.2%	4.2%	6.3%	5.4%	8.8%	10.7%	12.5%	15.9%	21.9%
	$\gamma + CF2$	1.3%	1.7%	4.3%	5.0%	5.2%	7.0%	12.0%	19.0%	55.0%

The influence of including a crossflow term on the propeller performance is exhibited in Figure 3, which shows the relative difference in the thrust and torque coefficients for each advance coefficient, when compared to the simulations without the crossflow term. The efficiency is depicted as well, and corresponds to the absolute difference between the simulations. Regardless of the crossflow term employed, lower K_T and K_Q are obtained across all J with the exception of the highest one. Regarding the efficiency, at $J = 0.34$ the simulations with crossflow modelling exhibit slightly higher efficiency, which decreases as J increases, resulting in an overall lower efficiency when a crossflow term is included. There is an exception to this at $J = 0.588$ for $\gamma + CF2$, which displays higher efficiency than the baseline simulation without crossflow. At the higher range of J, as a result of the higher thrust and torque for these conditions, the efficiency is also significantly higher than the one obtained in the baseline simulation.

Comparing the two different crossflow terms shows that for $J < 0.6$, the $\gamma + CF1$ model exhibits lower thrust and torque than $\gamma + CF2$. For $J > 0.6$, the situation changes, and instead the $\gamma + CF2$ model exhibits the lowest thrust and torque. On the other hand, the efficiency obtained with the $\gamma + CF2$ term is slightly higher than that of the $\gamma + CF1$ term up to $J = 0.75$. These trends indicate that the crossflow terms have a different influence at lower and higher advance coefficients.

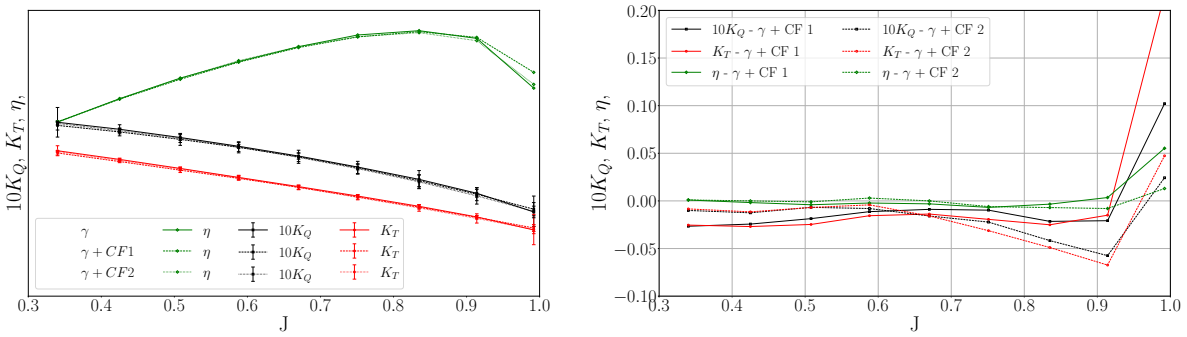

Fig. 3: Propeller open-water diagram for different transition modelling approaches (left) and relative difference of K_T, $10K_Q$ and η for the simulations with crossflow relative to the solution of the γ model for varying advance coefficient (right).

In order to illustrate this behaviour, Figure 4 displays the skin friction coefficient on the suction side of the blade at $J = 0.425$ for each of the transition modelling approaches, along with the limiting streamlines on the blade surface. If no crossflow term is employed, most of the flow over the surface of the blade is laminar, with a small turbulent region near the tip. The absence of turbulent flow leads to a significant region of separated flow near the trailing edge of the blade. Some differences in the extent of the turbulent region can also be observed between the simulations done with the crossflow terms, with the $\gamma + CF1$ model exhibiting a larger extent of turbulent flow. Although not shown here, for the same J, the pressure side of the blade exhibits transition over a small region near the tip of the blade at the trailing edge for $\gamma + CF1$, while fully laminar flow is obtained with the remaining approaches.

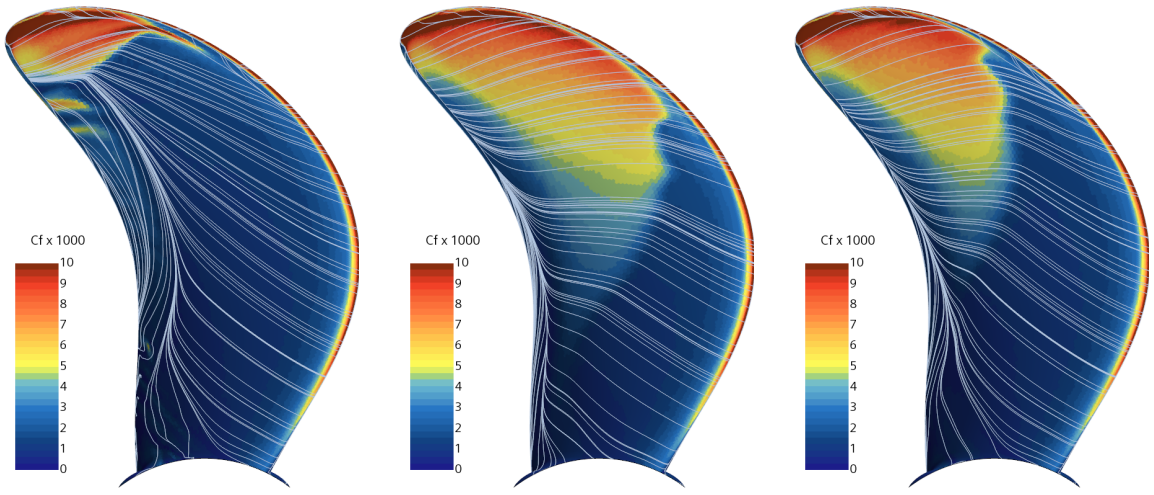

Fig. 4: Skin friction coefficient on the suction side of the propeller blade and limiting streamlines at $J = 0.425$ for the γ (left), $\gamma + CF1$ (middle) and $\gamma + CF2$ (right) models.

As the propeller is unloaded at higher advance ratios, the extent of the turbulent region on the suction side decreases, while increasing on the pressure side. This is illustrated in Figure 5, which depicts the skin friction coefficient on the pressure side of the blades for $J = 0.835$. Similarly to what was observed for the suction side at $J = 0.425$, the inclusion of a crossflow term leads to a larger extent of turbulent

flow and in this case prevents flow separation from taking place at the trailing edge. Once again, the $\gamma + CF1$ model leads to a larger extent of turbulent flow, as a consequence of earlier transition.

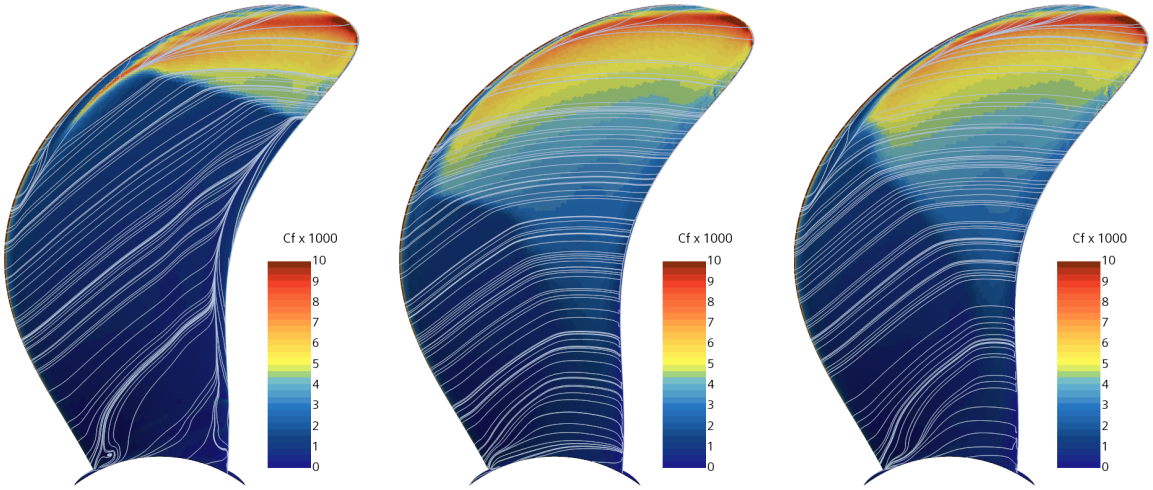

Fig. 5: Skin friction coefficient on the pressure side of the propeller blade and limiting streamlines at $J = 0.835$ for the γ (left), $\gamma + CF1$ (middle) and $\gamma + CF2$ (right) models.

5 Conclusions

Simulations of a controllable pitch propeller in an open water setup were performed at model scale, with three different transition modelling approaches in order to investigate the effect of crossflow transition on the propeller performance and flow field on the blade. The results show that if a crossflow term is not used, the flow over the propeller blades remains mostly laminar, leading to flow separation in some cases. Using a crossflow term causes a reduction in the extent of laminar and separated flow over the propeller blade, exhibiting better iterative convergence and a decrease in propeller thrust and torque, but not in efficiency. Although the two crossflow terms tested do not exhibit strong differences in the flow field, the difference in propeller performance obtained between them is as large as the difference to the simulations without a crossflow term, showing the importance of crossflow on predicted propeller performance. It is also observed that the larger extent of turbulent flow promoted by the $\gamma + CF1$ model leads to lower K_T and K_Q when the propeller is heavily loaded, but to higher thrust and torque as J increases.

Acknowledgements

This research is supported by Kongsberg Maritime Sweden AB through the University Technology Centre in Computational Hydrodynamics hosted by the Department of Mechanics and Maritime Sciences at Chalmers. The computations were enabled by resources provided by Chalmers e-Commons at Chalmers.

References

F. R. Menter, M. Kuntz and R. Langtry (2003). Ten Years of Industrial Experience with the SST Turbulence Model. *Turbulence, Heat and Mass Transfer 4*, 625–632.

L. Eça and M. Hoekstra (2014). A Procedure for the Estimation of the Numerical Uncertainty of CFD Calculations Based on Grid Refinement Studies. *Journal of Computational Physics*,**262** 104–130.

F. R. Menter, P. E. Smirnov, T. Liu and R. Avancha (2015). A One-Equation Local Correlation-Based Transition Model. *Flow, Turbulence and Combustion*,**95**(4) 583–619.

J. Baltazar, D. Rijpkema and J. F. de Campos (2018). On the use of the $\gamma - \tilde{R}e_{\theta_t}$ transition model for the prediction of the propeller performance at model-scale. *Ocean Engineering*,**170** 6–19.

C. Grabe, S. Nie and A. Krumbein (2016). Transition Transport Modeling for the Prediction of Crossflow Transition. AIAA Aviation Forum (AIAA 206-3572).

R. Lopes (2021). Simulation of Transition from Laminar to Turbulent Regime in Practical Applications of Incompressible Flow. PhD Thesis, Instituto Superior Técnico, Portugal